Forces in Mechanics 7 (2022) 100094

Contents lists available at ScienceDirect

Forces in Mechanics

journal homepage: www.sciencedirect.com/journal/forces-in-mechanics

Novel risk assessment tools for the climate-induced mechanical decay of wooden structures: Empirical and machine learning approaches

A. Califano [a,b], M. Baiesi [a], C. Bertolin [b,*]

[a] Department of Physics and Astronomy "Galileo Galilei", University of Padua, Padua, Italy
[b] Department of Industrial and Mechanical Engineering, Norwegian University of Science and Technology (NTNU), Trondheim, Norway

ARTICLE INFO

Keywords:
Hygro-mechanical stress
Wood
Microclimate
Machine learning
EN15757
Damage
Risk assessment tool

ABSTRACT

The microclimate in which historical buildings and objects are placed strongly influences the mechanical decay and properties of the constituent materials, especially if they are susceptible to fluctuations of temperature (T) and relative humidity (RH). For this reason, in this work, the attention is focused on the indoor microclimate of an historic building completely made of Scots pine wood: Ringebu Church (Norway). In particular, the indoor RH of Ringebu church has been analyzed by means of the European Standard EN15757, which establishes guidelines on assessing whether the RH fluctuations are risky for the conservation of historic hygroscopic materials (such as wood). However, for conservation purposes, it is useful to further study the entity of the RH fluctuations. In this framework, a novel simple strategy, named Median of Data Strategy (MoDS), for identifying RH drops is here proposed; the new approach, by scanning the RH time series and being tested on several examples, displays potential for better assessing the risk of degradation of wooden assets, objects, and artefacts. Then, based on evidence available in literature, a simple empirical model for computing the levels of hygro-mechanical stress developed due to hygric changes has been described and a novel tool for assessing the climate-induced mechanical risk for wooden structures has been proposed. Finally, a machine learning approach for predicting whether climatic fluctuations may have catastrophic effects on the historical wooden materials is presented as well. The obtained results show that the different proposed approaches may be useful for general assessments on the risk of decay of wooden samples and they open a pathway for future investigations in the fields of fracture mechanics, fatigue behavior and *smart* timeseries prediction for conservation and preservation purposes.

1. Introduction

Controlling the microclimate in historic heritage buildings is probably the most common conventional method for assessing their conservation state and preserving them from decay. In particular, in case of structural items and stored artefacts made by organic hygroscopic materials, the study of microclimate and its management is useful as preventive conservation technique for avoiding permanent deformation or, even worse, catastrophic failure. Among the existing organic hygroscopic materials, the attention is herein focused on wood and on wooden heritage buildings/objects, as they are highly susceptible to the thermo-hygrometric environmental variability; therefore, their risk of mechanical decay is tightly, but not exclusively, influenced by microclimate fluctuations [1,2]. These fluctuations may be caused by the natural microclimate variability experienced by the building/item or by the implementation of artificial Heating, Ventilation and Air Conditioning (HVAC) systems for ensuring precise levels of indoor comfort. In case of historical buildings, the installed HVAC systems are, generally, not sophisticated; this means that there are no adequate ways of controlling and mitigate the possible effects of temperature and relative humidity. In addition, in some cases (as those of historical churches, for instance) the HVAC systems are used only sporadically, causing short episodes of temperature (T) and relative humidity (RH) variations that have a negative impact on the wooden works of art and assets. For example, when the heating system is turned on in the cold periods of the calendar year, no moisture compensation is generally provided to the indoor environment. This results in a rapid warming of the air and in a significant drop of relative humidity that may have harmful effects on wooden objects, due to their hygroscopic nature. Therefore, the entity and the duration of the RH fluctuations strongly affect the risk of mechanical decay of wooden objects, items, and artefacts. For these reasons, establishing and following precise pathways on controlling and

* Corresponding author.
E-mail address: chiara.bertolin@ntnu.no (C. Bertolin).

https://doi.org/10.1016/j.finmec.2022.100094
Received 30 March 2022; Received in revised form 4 April 2022; Accepted 7 April 2022
Available online 9 April 2022

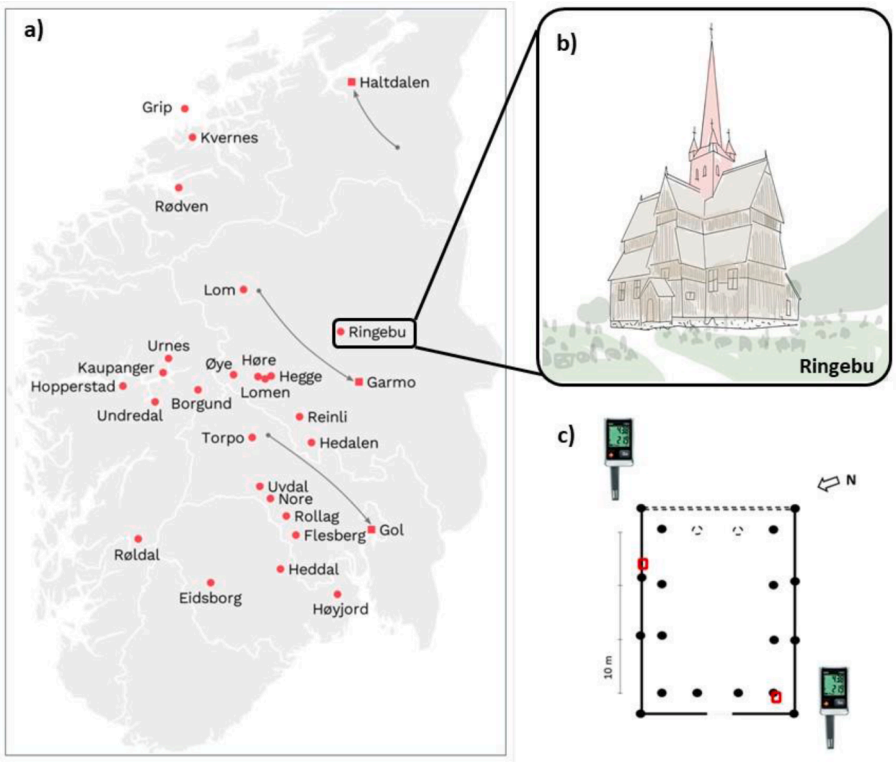

Fig. 1. Map of the Central-South Norway with the locations of the 28 still existing stave churches and the site of Ringebu stave church. Right - Ringebu Stave church (a), after Preserved stave churches in Norway by Store norske leksikon (https://snl.no/). Ringebu stave church: outdoor view (b) (drawn by Dr. Elena Sesana) and indoor view(c) with datalogger DL1 and DL2 highlighted in red.

managing the microclimate is fundamental to avoid the heritage properties undergoing unbearable thermo-hygric conditions. In this framework, long-term monitoring, simulations, and reliable risk-assessment tools are needed to quantify the threat level for the deterioration of artworks and artefacts, based on the influence that the climate may have on the indoor environment in heritage buildings. Andretta et al. [3] proposed a risk-assessment methodology, called NICHE, applied to monitored data in the Classense Library in Ravenna (Italy) and took in consideration the risk due to several possible microclimatic anomalous states; it was concluded that different classes of risk scenarios (CRSs) were distinguishable for each state, given that the microclimatic parameters agreed with the standards [4]. Another risk-based analysis was carried out using data collected inside the Milan Cathedral (Italy) [5]; it was observed that for wooden materials the optimal RH range was between 45% and 65%, mostly overlapping with the indications provided in the Italian Legislative Decree D. Lgs. 122/98 (art.150, par. 6) [6]. However, many risky periods and episodes were identified, during which both T and RH exceeded the suggested safe limits. Examples from monitoring campaigns are represented by the work of Silva and Henriques [7] which reports RH seasonal conditions and short-term fluctuations (in%) monitored in four churches available in literature *i.e.*, the Church of St Christopher in Lisbon (Portugal) [7]; the Church of St. Michael Archangel in Debno (Poland) [8], the Basilica of S. Maria Maggiore in Rome (Italy) [8] and the Church of S. Maria Maddalena in Rocca Pietore (Italy) [9]. This work specifies the allowable daily cycles as those defined by the 90th percentile of the recorded daily cycles if higher than the UNI 10,829 limits [10], and the seasonal cycles as those obtained by calculating a moving average of thirty days centered on the desire value and the short-term fluctuations as a target range calculated from the historic climate (*i.e.*, 5th and 95th percentiles of the short-term fluctuations over the monitoring period). Finally, they note two classes of risk of mechanical and biological decay, the former (low) applicable in museums buildings where the materials require tight control of climate levels; the latter (moderate) applicable in churches where there is no need of climate with constant levels and restrict fluctuations. Similarly, Varas-Muriel and Fort in 2018 [11] studied the impact of centralized heating system in the church of our lady of the Assumption in Algete (Spain) showing how within one hour of use, the air temperature reached the programmed level of 18 °C even in the upper heights of the church with RH drops ranging 20%−25% going below the target RH range for preventive conservation thus causing fissures and cracking on indoor assets. Bratasz [12] reports examples of stress fields, irreversible deformation, and fracture in wooden objects as panel painting and furniture which can be explained - under several forms of constraints - in terms of RH fluctuations. These visual damages are deformation on panels, cracks in wood, gesso, lacquer layer, or along joints, while in massive elements as sculpture obtained by cylindrical tree trunks, they are deep cracks in radial direction.

The correlation between outdoor and indoor climate has been highlighted and the risky fluctuations of RH according to EN15757 have been identified in [13] during the monitoring campaign organized in the Jeronimos Monastery in Lisbon (Portugal). The EN15757 was followed to compute the extreme percentiles (7th and 93rd) for the entire set of RH variations, in order to determine their *safe band* as stated in [14]. The two percentiles are fluctuating thresholds that faithfully follow the evolution of the climate and adapt to it, differently from the constant thresholds defined by D. Lgs. 122/98 (art.150, par. 6), EN16893:2018, ISO 19,815:2018 and ASHRAE standards [6,15–17]. Anaf and Schalm [18] applied the EN15757 to the 22-month monitoring campaign they performed in a chapel in the center of Antwerp (Belgium) controlled with a HVAC system. In their contribution they demonstrated how the analysis of T and RH peaks and drops could help in identifying hazards which caused fluctuations in different frequency ranges. Schellen and van Schijndel [19] presented the setpoint control for air heating in a church to minimize moisture related mechanical stress in wooden interior parts, using a HAMBase Simulink building model for simulating

the indoor T and RH and a COMSOL model for simulating dynamic moisture transport and related mechanical stresses in the monumental wood *i.e.* a lime wooden cylinder. Finally, they discussed the air T (and consequently RH) changing rate, showing that limiting the RH changing rate to 5% in one hour will preserve sensitive object from mechanical decay.

In this framework, the potential of EN15757:2010 is discussed in the current work, based on studies carried out on the microclimate of a Norwegian heritage building, Ringebu stave church, during the international Symbol – Sustainable management of heritage buildings in a long-term perspective- project (2018–2022). In detail, a discussion on whether the Standard works well as a control tool for mixed microclimates (natural and artificial) is presented. As a matter of fact, the EN15757:2010 defines guidelines on how to detect risky RH fluctuation but does not provide any indication on how to rank them in relation to hygro-mechanical stress. For this reason, the aim of this work is proposing approaches for assessing the climate-induced hygro-mechanical risk in wooden objects. First of all, a simple strategy, named Median of Data Strategy (MoDS), and a quick indicator for detecting and evaluating significant fluctuations in a time series have been proposed. Then, once the RH fluctuations have been detected through the MoDS, a simple empirical model for translating the RH variations into levels of hygro-mechanical stress is proposed. Then, the results have been used to build up a novel Risk Assessment Tool (RAT) for quick evaluations of the climate-induced mechanical risk in generic wooden samples. Several considerations have been highlighted, especially correlated with the distribution of stress over time, which can be assimilated to low-frequency fluctuation phenomena and, thus, can be in future evaluated in the framework of the climatic fatigue behavior of wood. This could be of extreme interest for carrying out successive evaluations about the arising and interaction of damage mechanisms on different length and time scales. Finally, a preliminary implementation of a machine learning classification model has been proposed to predict whether the RH fluctuations may lead to perilous outcomes (*e.g.*, failure). The current paper is structured as follows: in Section 2.1 the selected case study is presented, while in Section 2.2 the MoD strategy is explained and in Section 2.3 the empirical model for obtaining the levels of hygro-mechanical stress is obtained. The main results in terms of identified RH fluctuations are discussed in Section 3.1 with the novel RAT described in Section 3.2. Finally, the implemented machine learning model is presented in Section 3.3 and the main conclusions are highlighted in Section 4.

2. Materials and methods

2.1. Case study, data and metadata

The stave church that is object of this study is located in the south of Norway and it dates back to the beginning of the XIII century. In details, Ringebu church (Fig. 1) is located in the homonym municipality in the Inland region. The church was first mentioned in official documents in 1270.

As easily understandable from the word “stave”, the church is made of wood (Scots pine wood), and it has lasted until now thanks to several restorations that took place over the centuries. The main being the extension done by Werner Olsen in 1630–1632 in a cruciform shape and a last full restoration occurred in 1921 when the gallery above the entrance, and the ceiling of the nave were removed and the wall decoration from the 18th century was restored. Recently (2010–2015) during the Stave Church Preservation Programme (SCPP)[1] [20] the Norwegian Directorate for Cultural Heritage funded interventions to give the church new shingles and retarred and to carry on consolidation intervention on the indoor distempered painting in the chancel (2010–2011). In addition, the southern churchyard wall was repaired, and one stave was given a new foundation.

The main nave and the roof are supported by a total of 18 poles, while the wall logs in between these staves or poles are tucked into side bars and secured with wooden plugs. The corner poles are funded on stone slabs, while the wall logs on stone fill. Indoors, the internal pales in the single nave, support arc at double heights with on the top rods braced with Andrew`s crosses. The interior show wall paintings in blue and red colors decorated in 1719 that, with a unique (respect to the other distemper paints in the stave churches) drapery imitations, dominate the nave and the chancel. Two crucifixes are dated back to the Middle Age, to the first half of the 14th century. The two medieval crucifixes were treated at the start of the SCPP, but only one of them was returned to its medieval state, looking as it did before being painted over in the 18th century [20]. Inside the church, the altarpiece from the 1680s is the oldest object preserved since the Reformation; it is richly carved, gilded and colored with paintings, while the pulpit from 1703 is characterized by curved acanthus, a sort of hallmark of the folk art of the Gudbrandsdalen valley where the Ringebu stave church is located.

In light of the hygric nature of wood, that is the constituent material of both the building envelope and the numerous wooden pieces of art collected indoors, it is fundamental to study and analyze the microclimate of this building, to assess its possible impact on the durability of wooden items for cultural heritage and preservation purposes. In this framework, a monitoring campaign has been established within the Symbol project (n. 274,749) and further analyzed using machine learning within the Spara Och Bevara project (n. 50,049–1). Ringebu stave church has been equipped with three dataloggers each (named DL1, DL2 and DL3), that collect temperature (T) and relative humidity (RH) data. The DL1 and DL2 are located indoors and have a data acquisition rate of 5 min, while DL3 is located outdoors and has a data acquisition rate of 15 min. The set of dataloggers has been installed on March 30th 2019 and they have been collecting data since their installation. Collecting T and RH data is allow understanding the evolution of the microclimate of the case study; in this case, the microclimatic data are useful to analyze the cycles of heating/de-heating and dehumidification/humidification that the church and the wooden piece of art undergo in the period of observation. It has to be highlighted that artificial heating systems are installed in Ringebu Church in the form of traditional radiators. In a typical calendar year, Ringebu church is heated from half September to half April and the heating is sporadically turned on only in case of scheduled events (weddings, services, funerals *etc.*); in detail, the heating is turned on several hours before the start of the event and it is turned off when the event ends, in order to keep the indoor environment comfortable for churchgoers. Together with the microclimatic data of T and RH, information about the use of the church has been collected as well. These are mostly metadata about scheduled events (type of event and time) and the number of people attending the events themselves. From these data it is possible to get information about the occurrence of the events and their duration that, crossed with the T and RH data, is useful for successive analysis.

2.2. Strategy for the identification of relative humidity drops

The main issue of using artificial heating is linked to periods of forced drying induced by the dehumidification of the indoor environment without moisture content compensation; this may cause permanent mechanical damage or failure of the wooden objects, if not controlled properly. This is why this work aims to propose a strategy to identify and evaluate the RH variations. According to the standard EN15757, useful indicators for the evaluation of the indoor climate are the target values and the target range of RH. The target values of RH are obtained evaluating the central moving average (MA) over 30 days, while the target range is determined as the band confined between the 7th and the 93rd percentiles of the RH fluctuations, respect to the moving average of RH,

[1] Reports on the SCPP, in Norwegian, available at: https://ra.brage.unit.no/ra-xmlui/handle/11250/176302?locale-attribute=en

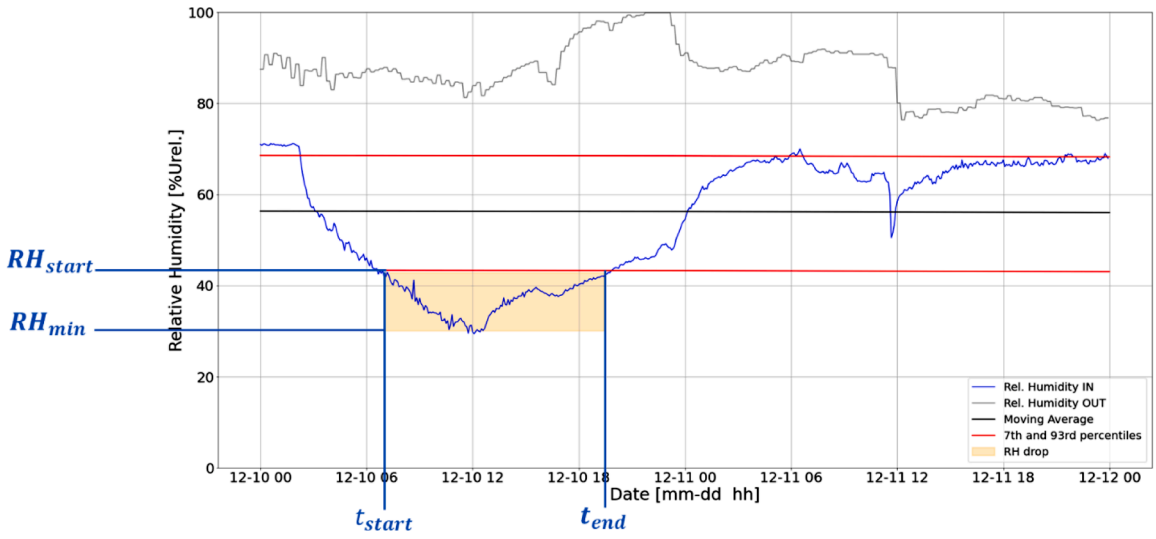

Fig. 2. Ringebu Church: identification of an RH drop and of the quantities defined in Eqs. (4) and (5).

during the monitoring period. This band is known as *safe band,* because it represents the range where RH fluctuations are classified as non-risky. Hence, dangerous RH fluctuations exceed the safe band [14]. This condition is likely to take place in case of use of heating systems, as the RH level dramatically drops. Quantities as indoor T, outdoor T, indoor RH (together with its MA and percentiles) and outdoor RH are reported in the Appendix for Ringebu Church. From now on, all the evaluations will be referred to the same period of observation, *i.e.*, two years (from March 2019 to March 2021). Analyzing Fig.A1 in the Appendix, it is clear that, especially when the sporadic heating is used, the safe band of RH is often exceeded due to over dryings of the environment. For this reason, a useful strategy consists in identifying all the cases in which the lower bound (namely, the 7th percentile curve) of the safe band is crossed and exceeded by the RH readings. This is possible by defining and comparing the following quantities:

$$\Delta RH_{act} = RH_{measured} - RH_{MA} \tag{1}$$

$$\Delta RH_{safe} = RH_{lowerbound} - RH_{MA} \tag{2}$$

where ΔRH_{act} is the difference between the actual considered RH reading ($RH_{measured}$) and the respective RH value coming from the central moving average for the same day (RH_{MA}), representative of the actual measured *anomaly* respect to the central moving average calculated over 30 days; ΔRH_{safe} is the difference between the RH value coming from the 7th percentile curve for the same day ($RH_{lowerbound}$) and RH_{MA}. If the following reasonable condition

$$\Delta RH_{act} < 0 \wedge |\Delta RH_{act}| > |\Delta RH_{safe}| + 1\% \tag{3}$$

at some point is met, it means that the safe band is exceeded due to dehydratation. According to this logic, as soon as the RH curve crosses the lower bound curve from above, it means that the RH is moving towards low values (considered risky by the Standard), most likely because the artificial heating has been turned on. While the heating is on, RH continues to decrease until it reaches a local minimum that is representative of the maximum level of dryness caused by the artificial heating. As soon as the heating is turned off, the RH usually starts to increase from its minimum until it re-enters the safe band. In this way, it is possible to identify the period during which the RH is in the risk area and to evaluate the minimum value reached in that selected period, RH_{min}. At this point, the amount of RH exceeding the lower percentile, named RH_{risky} for the sake of simplicity, may be evaluated as follows:

$$RH_{risky} = RH_{start} - RH_{min} \tag{4}$$

Table 1
Details about the RH drop identified in Fig. 2.

RH_{risky}	RH_{min}	RH_{start}	t_{start}	t_{end}
15%	30%	45%	Dec 10th at 7:00	Dec 10th at 19:30

where RH_{start} is the first value of RH that satisfies the condition (3) at the beginning of the RH drop. In addition, the duration of the RH_{risky} is calculated as follows:

$$\Delta t_{risky} = t_{end} - t_{start} \tag{5}$$

where t_{start} is the time when RH_{start} is measured, and $t_{end}$is the time when the last value, RH_{end}, satisfying the condition (3) is measured. For the sake of clarity, Fig. 2 illustrates graphically the quantities defined above, representing a time window from December 10th 2019 to December 12th 2019. A RH_{risky} of almost 20% is highlighted with an orange box.

From the metadata of Ringebu church, it is extrapolated that on December 10th 2019 at 11:00 a one-hour funeral took place. This means that the heating had been turned on several hours before the event and that it had been turned off at the end of the funeral itself, *i.e.*, at 12:00. In fact, looking at Fig. 2, it is clear that RH_{min} of about 30% is reached at 12:00, while, according to this strategy, RH_{start} of about 45% is measured at 7:00. A summary of this information is reported in Table 1.

However, looking in detail at Fig. 2, it can be seen that the RH (blue curve) starts decreasing way before the time selected with this strategy (t_{start} = 7:00). This means that the heating has been turned on before 7:00 and that the actual RH drop experienced within the church is way higher than the RH_{risky} shown in Fig. 2.

From a naked-eye analysis of Fig. 2, it may be highlighted that the actual RH drop is of about 40%, being the actual RH_{start} of roughly 70%. This simple example shows that the standard EN15757, by detecting only the risky amount of RH, may not be useful for practical applications dealing with active indoor climate control because it does not provide guidelines about how detecting the total actual drops of RH experienced by the wooden elements/structural items. For this reason, a new strategy is herein proposed. It uses a simple algorithm summarized in the flowchart in Fig. 3, based on scanning the entire dataset with fixed-length time-windows. In this case, the data scanning is carried out with a time-window of one hour length (*i.e.,* time-window with $L = 12$ readings, being the indoor reading acquisition rate of 5 min). The main steps of the algorithm are described as follows:

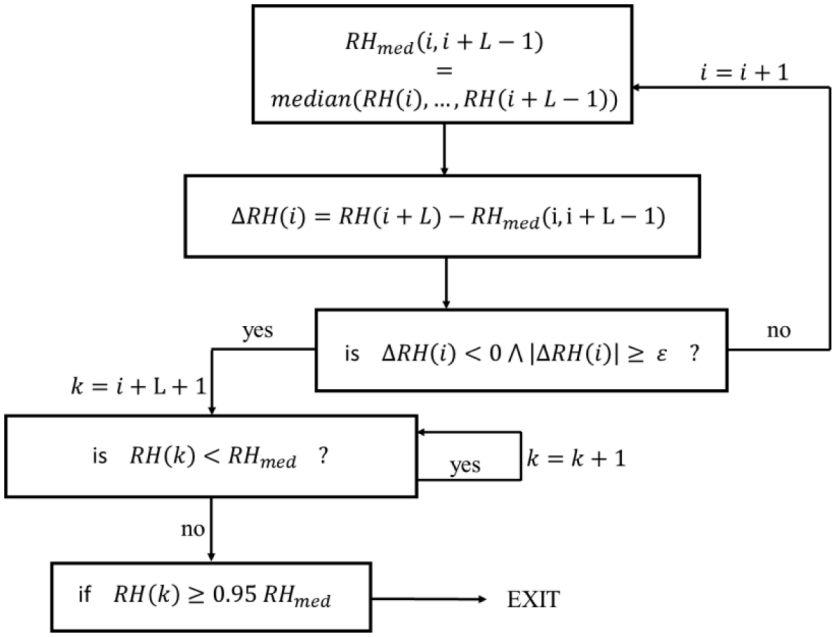

Fig. 3. Flowchart of the proposed strategy based on the evaluation of the median of data.

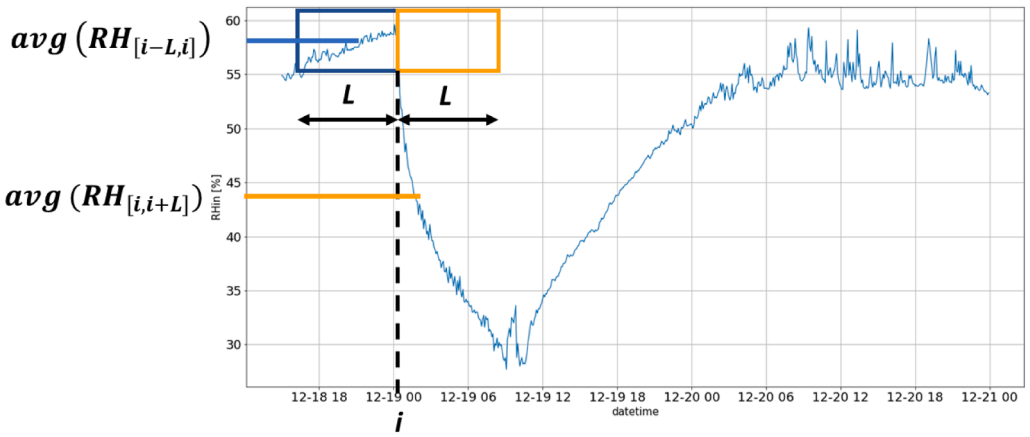

Fig. 4. Chunk of indoor RH (blue curve) on which two subsequent time-windows have been selected (blue and orange rectangles). Each window of data is characterized by an average level of RH (blue and orange horizontal line respectively).

- the median of data (RH_{med}) is evaluated on the values from $RH(i)$ to $RH(i+L-1)$;
- the following value, $RH(i+L)$, is compared to the just computed median in terms of distance, $\Delta RH(i)$;
- if the distance is negative ($\Delta RH(i) < 0$), it means that the trend of RH is decreasing. In addition, if the absolute value of this distance exceeds a given threshold ($|\Delta RH(i)| \geq \varepsilon$), it means that RH is moving towards a local minimum (*i.e.*, the RH is dropping). The threshold (ε) is set at 2% as it has been noticed that, in case of use of artificial heating, RH varies of about 2% in one hour;
- as soon as the threshold is exceeded, the RH drop starts, and RH keeps on decreasing ($RH(k) < RH_{med}$);
- as soon as the RH goes back to values that are near the previously calculated median ($RH(k) \geq 0.95\, RH_{med}$), it means that the drop has ended as RH has gone back to a stable behavior (*i.e.*, without the perturbation caused by heating);
- once the set of data constituting the entire RH drop has been identified, it is easy to determine RH_{start} and RH_{min} for the drop itself.

Using this simple logic, it was possible to detect and highlight the actual drops experienced by the relative humidity due to the use of artificial heating in cold months. Moreover, setting a different threshold (1%) in the flowchart in Fig. 3, it has been possible to detect the natural RH drops taking place during the warm months due, mainly, to the natural outdoor climate. In this way, a database containing the information about RH drops has been built up.

The procedure highlighted in Fig. 3 allows to detect the RH drops and to quantify their entity by collecting information like RH_{start}, RH_{min} etc. However, if, for some reason, there is the need to simply detect the occurrence of RH fluctuations neglecting any kind of detail, a quick and simple *ad-hoc* indicator, proposed in the following, can be used. Fig. 4 shows a chunk of indoor RH timeseries represented by a blue curve. Along the timeseries, two subsequent time-windows (blue and orange rectangles) of length L can be considered. As they are adjacent, they share the i point of the timeseries; in particular, the first time-window (blue rectangle) covers the range of data going from RH_{i-L} to RH_i, while the second time-window (orange rectangle) covers the range of data going from RH_i to RH_{i+L}. The average level of RH for each window of data can be computed: $avg\,(RH_{[i-L,i]})$ for the first time-window (blue horizontal line in Fig. 4) and $avg\,(RH_{[i,\ i+L]})$ for the second time-window

Table 2
Data obtained through the experiments carried out in [21].

Observation n.	ΔRH [%]	Stress [MPa]
1	0.5	0.27
2	5	2.06
3	10	3.36
4	20	5.56
5	30	7.53
6	40	9.39

(orange horizontal line in Fig. 4). As a fluctuation of RH is characterized by an abrupt variation of the general trend of RH, the following quantity can be introduced

$$V_i = avg\ \left(RH_{[i-L,i]}\right) - avg\ \left(RH_{[i,\ i+L]}\right)\ i = 1 + L,\ \cdots,\ N_{data} - L \tag{6}$$

where N_{data} is the number of data in the timeseries. The quantity in (6) can be introduced as useful tracer for the occurrence of RH drops. The results in terms of V_i computed on different-length time-windows are reported in Section 3.1.

2.3. Model for the quantification of the developed hygro-mechanical stress

Once the information about the experienced RH drops has been collected, the following step consists in trying to quantify the hygro-mechanical stress caused by such hygric fluctuations. To do so, observations and evidence available in literature have been exploited. In [21], experiments on circular slices of Scots pine were carried out. The wooden slices were conditioned in a climate chamber at 80% RH to reach the equilibrium with the chamber environment and then, a sudden change in RH up to 30% was introduced. The acclimatization period caused the formation of stress fields and macro cracks that have been evaluated at different steps throughout the experiment. The results in terms of hygro-mechanical stress and RH drops at which those stresses have been observed for a standard slice of Scots pine (diameter = 16 cm, thickness = 2 cm) are reported in Fig. 6a in [21] and summarized in Table 2. Due to the limited amount of experimental data and to a deep lack of similar evidence in literature, the results in [21] together with the results proposed by Jackiela et al. [22] for a standard cylindrical element of lime wood (diameter = 13 cm) have been used as ground truth for building up a simplified model for quantifying the hygro-mechanical stress levels caused by the RH drops. According to [22], it has been seen that the behavior of Lime wood in terms of hygro-mechanical stress *vs*. initial RH (experienced at the beginning of the RH drop) is well-defined trough quadratic curves. Due to the physics behind the simulations and results obtained in [22], it is reasonable to assume that this behavior, with the right adjustments and adaptations, is qualitatively valid for any kind of wood subjected to RH variations.

Starting from this assumption, the parameters *a, b* and *c* for each of the quadratic curves in [22] have been extrapolated by a simple curve fit of

$$y = aX^2 + bX + c \tag{7}$$

where y = Stress [MPa] and X = initial level of RH. Once the parameters *a, b* and *c* have been obtained for each curve (one curve for each RH drop, *i.e.*, ΔRH, evaluated in [22]), their trend with the RH drop has been evaluated and it is plotted in Fig. 5.

It has been seen that the trend of *a, b* and *c* with ΔRH is quadratic as well, and it can be formulated as follows

$$a = \alpha_a x^2 + \beta_a x + \gamma_a\ b = \alpha_b x^2 + \beta_b x + \gamma_b\ c = \alpha_c x^2 + \beta_c x + \gamma_c \tag{8}$$

where $\alpha_i,\ \beta_i$ and γ_i with $i = a,\ b,\ c$ are the quadratic fitting parameters and x is the experienced ΔRH. If the set of Eq. (8) is defined, it is possible to compute the parameters *a, b* and *c* for a given experienced ΔRH (x) and then, by substituting *a, b* and *c* in Eq. (7), to find the related hygro-mechanical stress (σ) developed after experiencing the selected ΔRH, started at a given level of RH (X). As Ringebu church is almost entirely made of Scots pine wood, the experimental observations in [21] can be used to tailor the empirical procedure expressed through Eq. (7)-8 on this considered type of wood. As in the experiments the wooden slices were conditioned at 80% RH to be in full equilibrium with the surrounding environment, this initial level of RH will be assumed to be characterized by the absence of forces within the wooden objects. This means that the quadratic curves representing the trend of the hygro-mechanical stress with respect to the initial RH will have their minima at initial RH equal to 80%. For this purpose, the quadratic curves obtained with Eq. (7)-8 manipulating those from [22] need to be translated accordingly. The generic equations for translating the points of the *i th* curve of the quantity (x_{0i}; y_{0i}) on a *xy* plane are the following

$$\begin{cases} x^{'} = X + x_{0i} \\ y^{'} = Y + y_{0i} \end{cases} i = 1,\ \cdots,\ n \tag{9}$$

where n is the total number of curves, X and Y are the coordinates of points before the translation and $x^{'}$ and $y^{'}$ are the coordinates of the points after the translation. This means that the *i th* translated curve will be obtained by substituting Eq. (9) in Eq. 7.

$$y^{'} - y_{0i} = a(x^{'} - x_{0i})^2 + b(x^{'} - x_{0i}) + c\ i = 1,\ \cdots,\ n \tag{10}$$

By carrying out all the mathematical steps, the final equation for the translated *i th* quadratic curve can be obtained

$$y^{'} = a_{new,\ i}x^{'2} + b_{new,\ i}x^{'} + c_{new,\ i}\ i = 1,\ \cdots,\ n \tag{11}$$

where

$$\begin{cases} a_{new,i} = a \\ b_{new,i} = b\ - 2ax_{0i} \\ c_{new,i} = a{x_{0i}}^2 - bx_{0i} + c + y_{0i} \end{cases} i = 1,\ \ldots,\ n \tag{12}$$

In the current case, as the horizontal translation of the curves consists in moving their minima from RH = 50% (see [22]) to RH = 80% (see [21]) (for each curve), the quantity x_{0i} is

$$x_{0i} = 80\% - 50\% = 30\%\ \forall i \tag{13}$$

while, concerning the y_{0i}, as in the σ-*RH* plane it is related to the

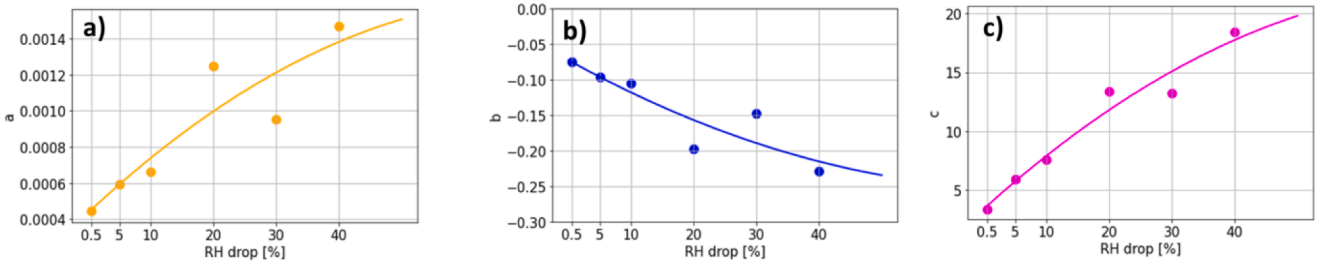

Fig. 5. Trend of the quadratic fitting parameters: a (a), b (b) and c (c) with respect to the RH drop as extrapolated from [21].

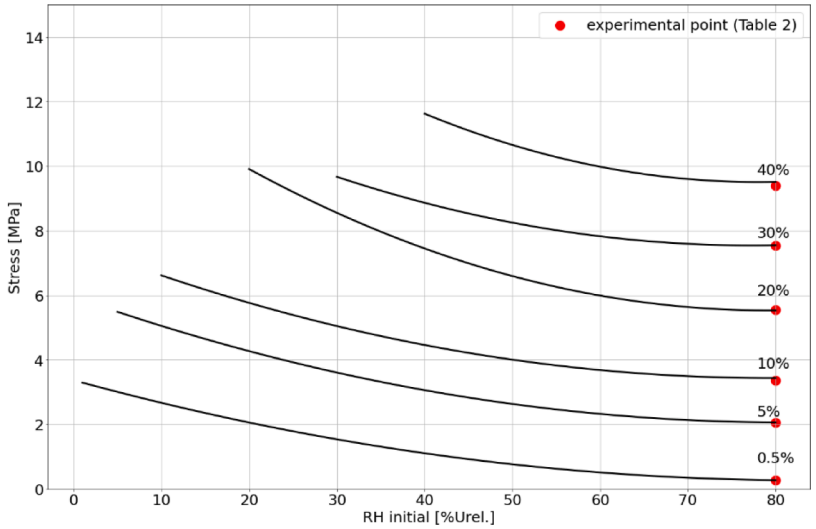

Fig. 6. Graphical representation of the model described through Eq. (7)-14 based on evidence in [21]. The black curves represent the quadratic trend of the hygro-mechanical stress with respect to the RH value at the beginning of a drop. The red circles are the experimental data obtained in [21] and summarized in Table 2.

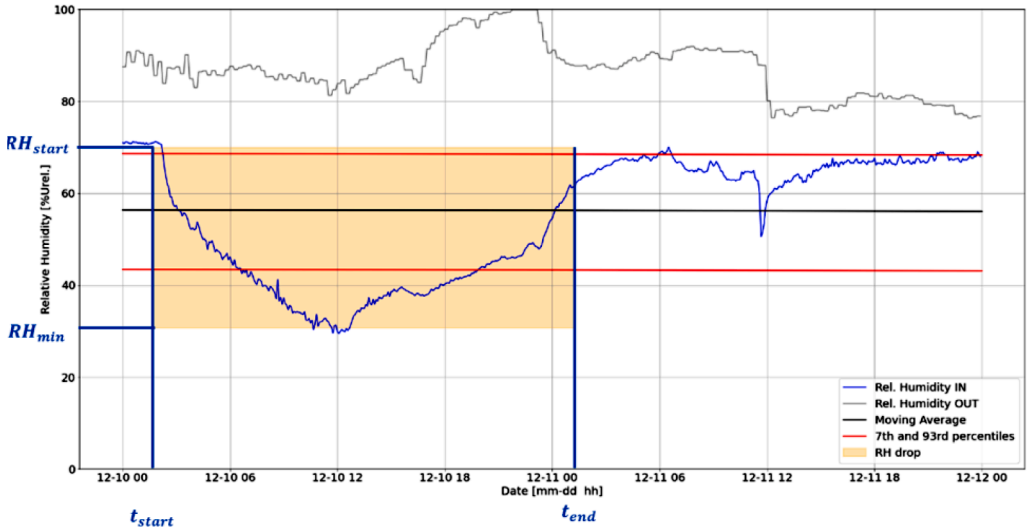

Fig. 7. Identification of an RH drop using the strategy summarized in Fig. 3.

minimum level of hygro-mechanical stress for each curve, it is

$$y_{0i} = \sigma_{\min,i_{Bertolin}} - \sigma_{\min,i_{Jackiela}} \quad i = 1, \cdots, n \tag{14}$$

where $\sigma_{min,i_{Bertolin}}$ and $\sigma_{min,i_{Jackiela}}$ are the minimum stress levels for the *i th* curve (*i.e.*, for the *i th* ΔRH) obtained through the experiments in [21] and the simulations in [22], respectively. At this point, based on simplifying assumptions, the set of Equations from 7 to 14 allows to design a model for easily and qualitatively assessing the level of hygro-mechanical stress experienced by the wooden objects due to the hygric variations, graphically shown in Fig. 6. The black curves are the graphical representation of Eq. (11), while the red circles are the experimental data obtained in [21] and summarized in Table 2, which are used as ground truth for building up the model described so far.

Table 3
Details about the RH drop identified in Fig. 7.

	RH_{min}	RH_{start}	t_{start}	t_{end}
40%	30%	70%	Dec 10th at 1:30	Dec 11th at 1:00

3. Results and discussion

The previous Sections have dealt with the description of the case study, the definition of a simple algorithm that is able of detecting the drops of relative humidity, and the design of a simplified methodology to assess the level of hygro-mechanical stress experienced by wooden objects. The following Sections present the main results in terms of: i) identification of RH drops with the previously presented procedure (Section 3.1); ii) quantification of the hygro-mechanical stress levels associated with the hygric variations and description of a novel Risk Assessment Tool (RAT) for determining the risk of microclimatic mechanical decay of wooden elements (Section 3.2).

3.1. Identification of the relative humidity drops

An example of the detected drop is reported in Fig. 7, showing the same period chosen for Fig. 2; additional details are reported in Table 3. Comparing these plots, it can be highlighted how the new strategy is able to better identify the RH drop, avoiding the underestimation

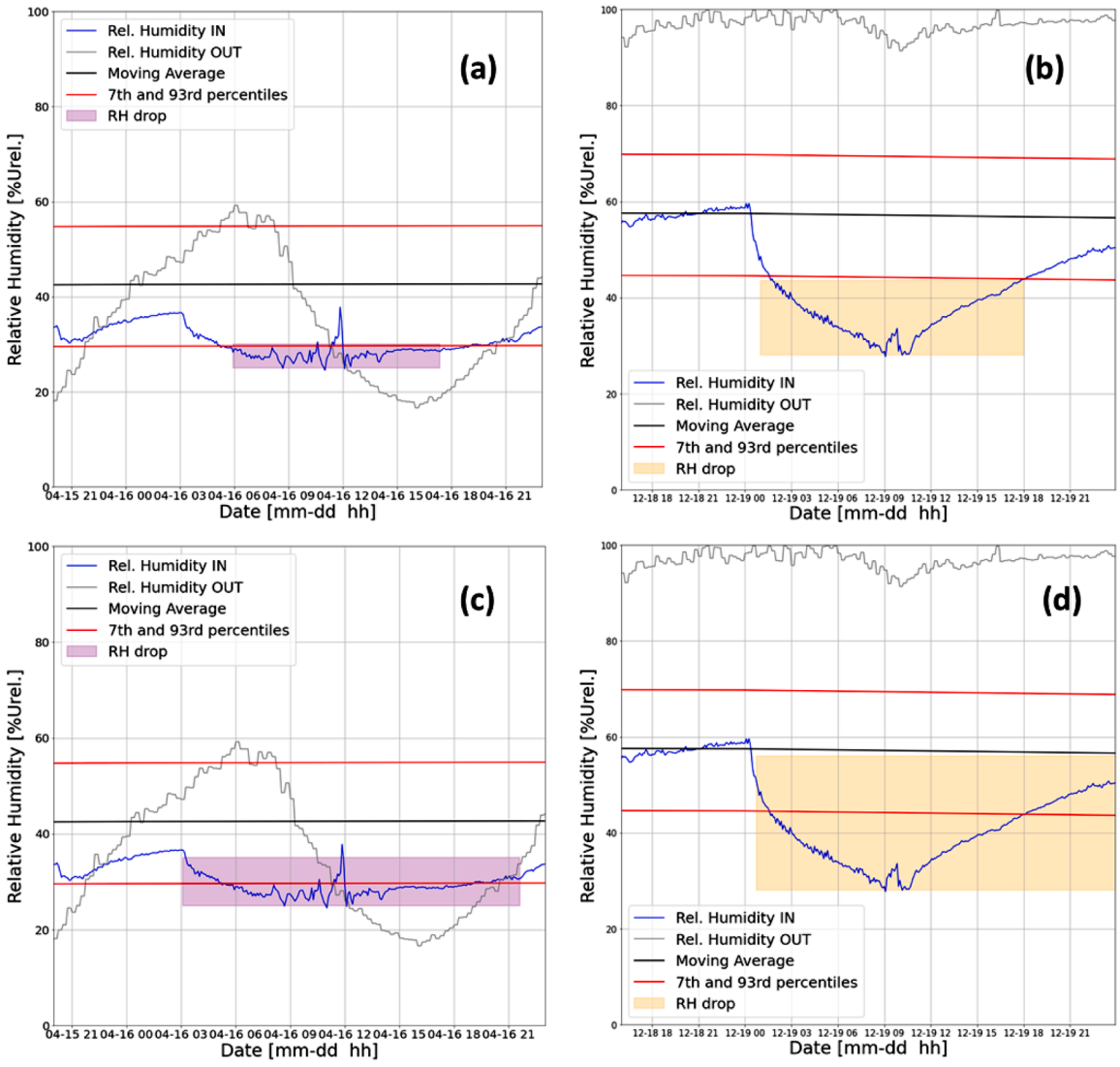

Fig. 8. Identification of two different RH drops in Ringebu church: the first drop identified with the EN15757 (a) and the novel median strategy (c); the second drop identified with the EN15757 (b) and the novel median strategy (d).

provided by the only use of the standard EN15757. In this case, the use of the Standard as unique tool to rely on would have led to the detection of RH_{risky} that is almost the 37% of the actual entire RH_{drop} detected with the new strategy. This simple strategy underlines that, although the European Standard has an indisputable importance for general assessments on the natural microclimate inside heritage buildings, it has an actual limited applicability because nowadays the majority of buildings - here included the historic ones – have HVAC systems in operation. As shown with practical examples, based on how the target range of RH is defined in the EN15757, it could underestimate significant portions of the RH variations and fluctuations that, instead, could have a severe impact on the wooden objects, assets, and artefacts. Further examples are reported in Fig. 8.

In particular, Fig. 8a and Fig. 8c show the identification of an RH fluctuation on April 16th 2019 in Ringebu Church with both strategies explained before. While Fig. 8b and Fig. 8d show the identification of an RH fluctuation on December 19th 2019. Details of the identified fluctuations with both strategies are reported in Table 4.

It may be seen how the RH_{risky} detected on April 16th 2019 is almost 50% of the actual RH_{drop}, while the RH_{risky} detected on December 19th 2019 is almost the 60% of the actual RH_{drop}. The three examples shown in Figs. 2, 7-8 represent, respectively, situations where RH starts near: 1) the upper part of the safe band; 2) the lower part of the safe band; 3) the center of the safe band. A summary of the three examples is shown in Table 5. The first three columns report the Figures and RH Position for

Table 4
Details of the identified RH fluctuations showed in Fig. 8.

	April 16th 2019		December 19th 2019	
	EN15757	Median	EN15757	Median
RH fluctuation	RH_{risky}= 5%	RH_{drop}= 10%	RH_{risky}= 17%	RH_{drop}= 29%
RH_{min}	25%	25%	28%	28%
RH_{start}	30%	35%	45%	57%

Table 5
Summary of the examples shown in Figs. 2,7 and 8 and Tables 1, 3 and 4.

	Figure	Position of RH profile	$\frac{RH_{risky}}{RH_{drop}}$
Example 1	2, 7	High percentile	37%
Example 2	8(a), 8(c)	Low percentile	50%
Example 3	8(b), 8(d)	Moving Average	60%

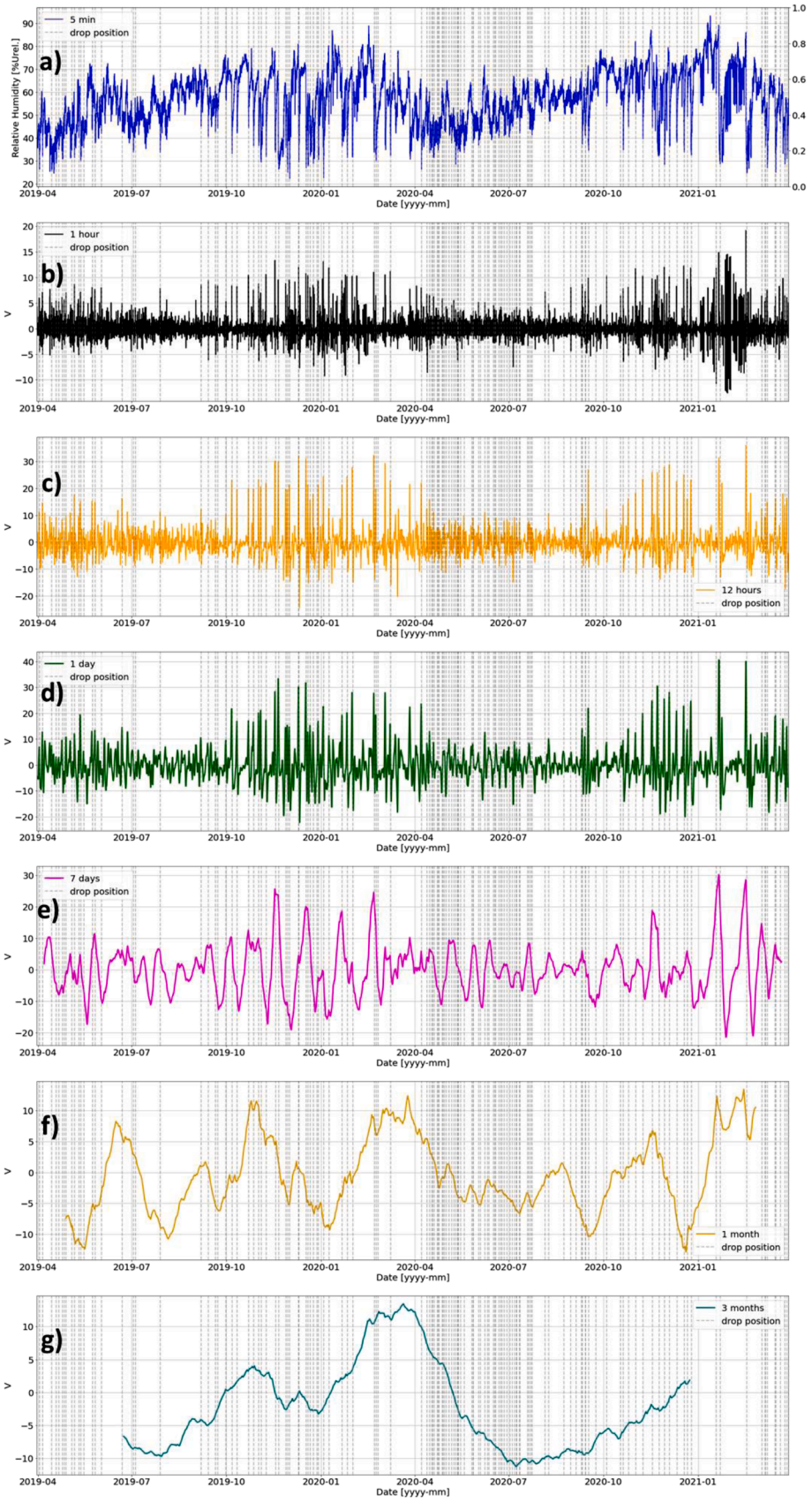

Fig. 9. Original indoor RH timeseries (a) and V timeseries (Eq. (6)) computed on different-length time-windows: one hour (b), twelve hours (c), one day (d), seven days (e), one month (f) and three months (g). The gray dashed lines represent the occurrence of RH drops identified with the procedure presented in Section 2.2.

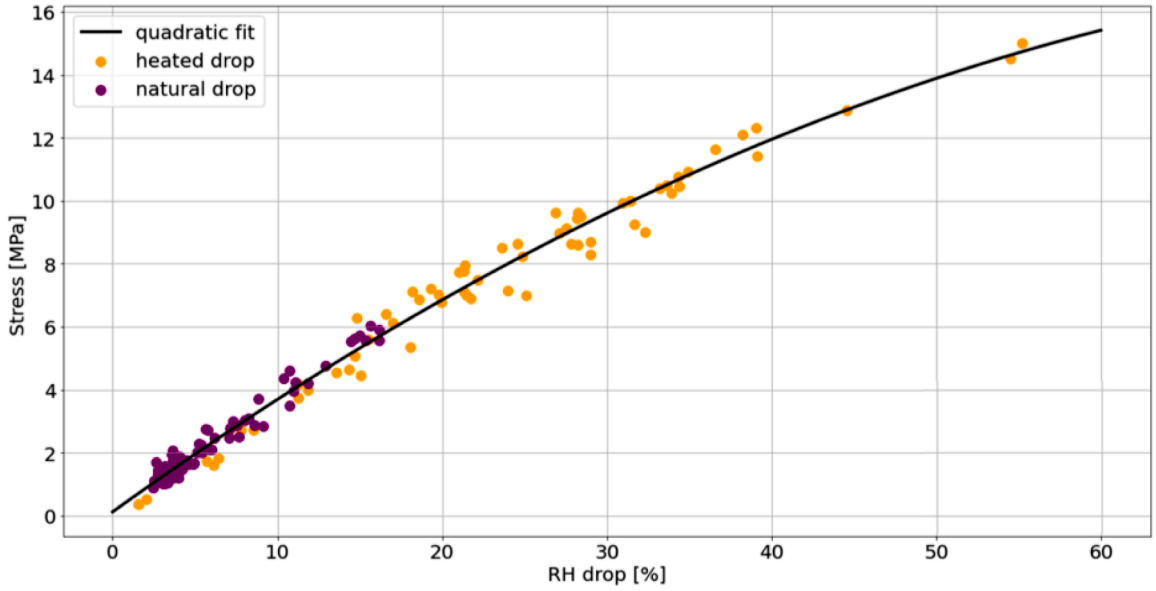

Fig. 10. Hygro-mechanical stress associated with each of the RH drops (natural – purple dots, artificial – orange dots) identified in the measured indoor RH timeseries of Ringebu Church. The quadratic trend is highlighted through the black curve.

each of the three previous examples, while the fourth column reports the quantity $\frac{RH_{risky}}{RH_{drop}}$, which represents the portion of RH_{drop} that falls outside the *safe band* of RH fluctuations.

From Table 5, it can be deduced that if the RH profile is near the high percentile, it might happen that almost the entire drop of RH is *masked* by the safe band and only a small portion of the drop itself is considered *risky*, according to the Standard EN15757. This further proves that detecting only the RH_{risky} portion is not representative of the actual behavior of the relative humidity. Following the strategy in Fig. 3, the drops of RH in Ringebu church have been detected and identified with a reasonably good precision.

Moreover, to have a further indicator and tracer for the occurrence of RH drops, the quantity V_i defined in Eq. (6) has been computed considering different-length time-windows. The results are shown in Fig. 9 for time-windows of the following lengths: one hour (Fig. 9b), twelve hours (Fig. 9c), one day (Fig. 9d), seven days (Fig. 9e), one month (Fig. 9f) and three months (Fig. 9g). In addition, the original indoor RH timeseries, characterized by a sampling time of five minutes, is shown in Fig. 9a. In each subplot of Fig. 9 the gray dashed vertical lines represent the position of the RH drops identified with the algorithm presented in Section 2.1. From Fig. 9 it can be highlighted that the spikes of V computed on time-windows of one hour, twelve hours and one day are overlapping with the actual drops detected in the RH timeseries. Moreover, the peaks and valleys of V computed on wider time-windows (seven days, one month and three months) comprise several closely spaced RH drops, providing a preliminary and qualitative tracer of the cumulative effect of subsequent drops.

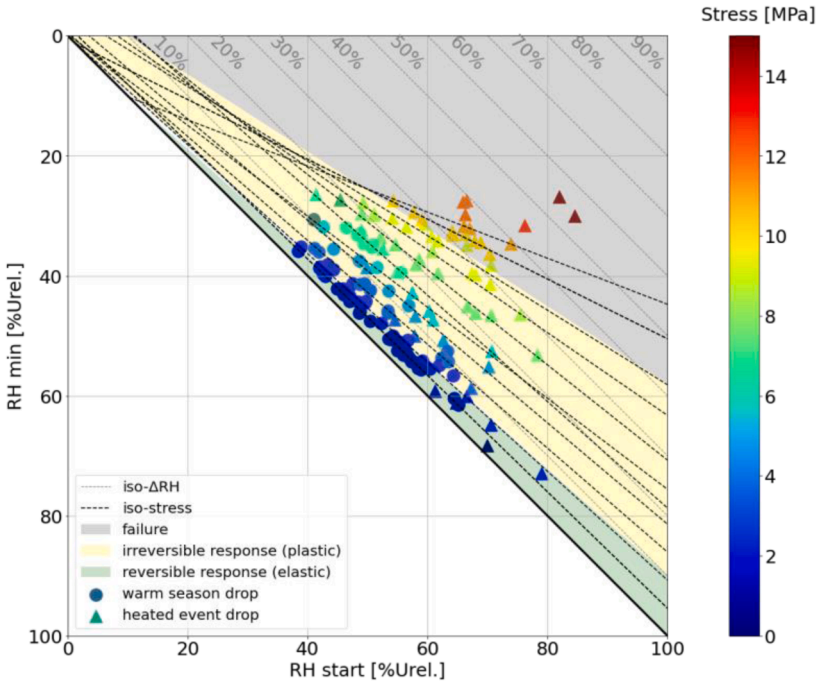

Fig. 11. Novel RAT for the evaluation of climate-induced mechanical risk of Scots pine samples. The gray dotted lines are iso ΔRH lines, while the black dashed lines are isostress lines. The scatters represent the identified drops (natural - circles, artificial – triangles) identified with the MoD strategy and the colors represent the entity of the developed hygro-mechanical stress levels computed following the empirical method in Section 2.3. Colors are referred to the color bar on the right. The green, yellow and gray zones represent the areas of reversible (elastic) response, irreversible (plastic) response and failure respectively.

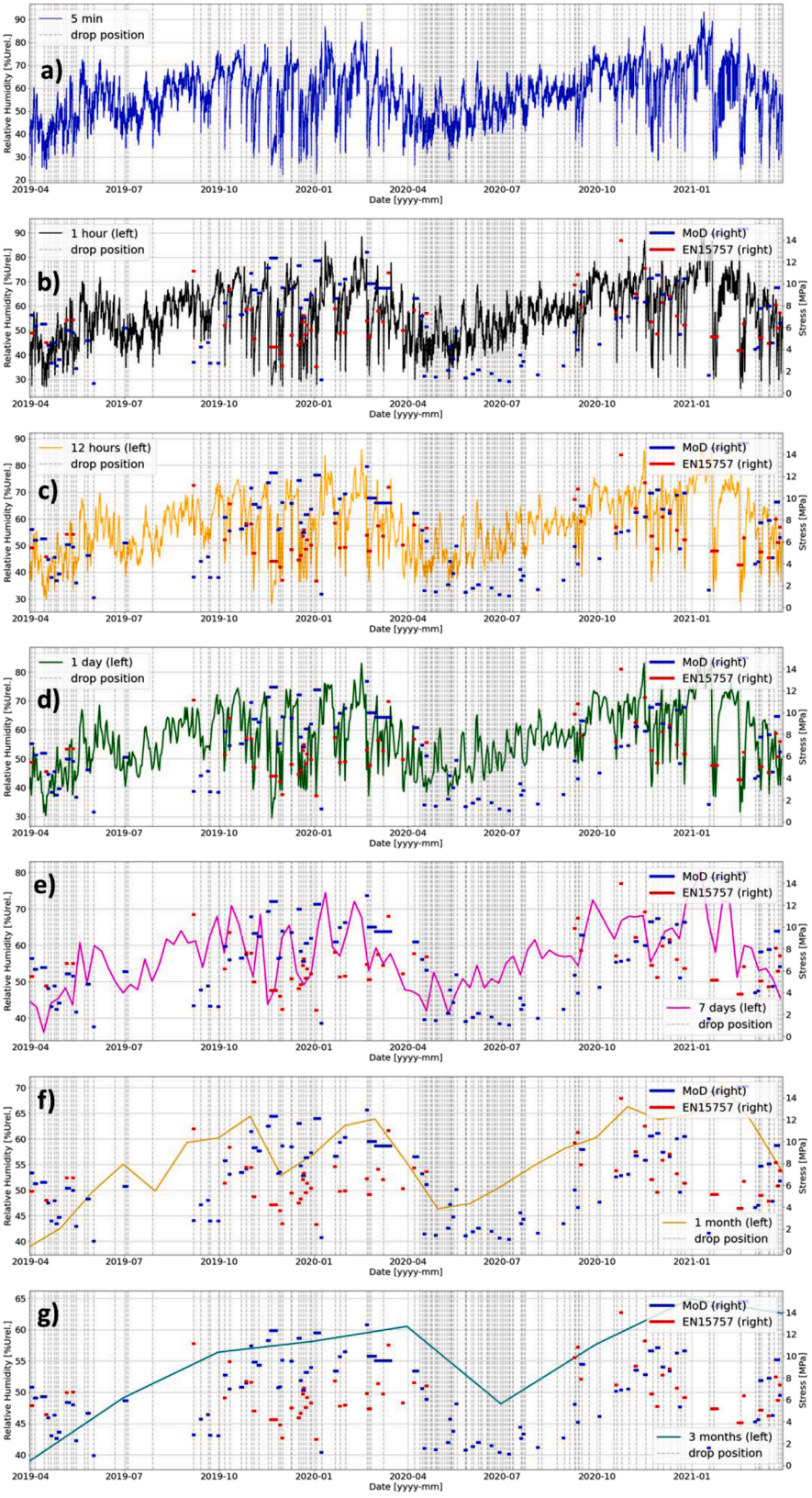

Fig. 12. Original indoor RH timeseries (a) and hygro-mechanical stress levels computed through the model in Section 2.3 for RH drops identified with the MoD strategy (blue segments) and with the EN15757 (red segments). The stress levels have been plotted over the RH timeseries resampled at the following frequencies: one hour (b), twelve hours (c), one day (d), seven days (e), one month (f) and three months (g). The gray dashed lines represent the occurrence of RH drops, as in Fig. 9.

3.2. A novel risk assessment tool for the hygro-mechanical decay of wooden elements

After having identified the RH drops through the MoD strategy (Section 2.2 and Section 3.1), the empirical methodology described in Section 2.3 may be useful for qualitatively evaluating the level of hygro-mechanical stress related to the experienced variations of RH. Following the steps and the equations previously introduced, the level of stress for each RH drop identified in the indoor RH timeseries monitored in Ringebu church has been computed. The trend of the stress levels with

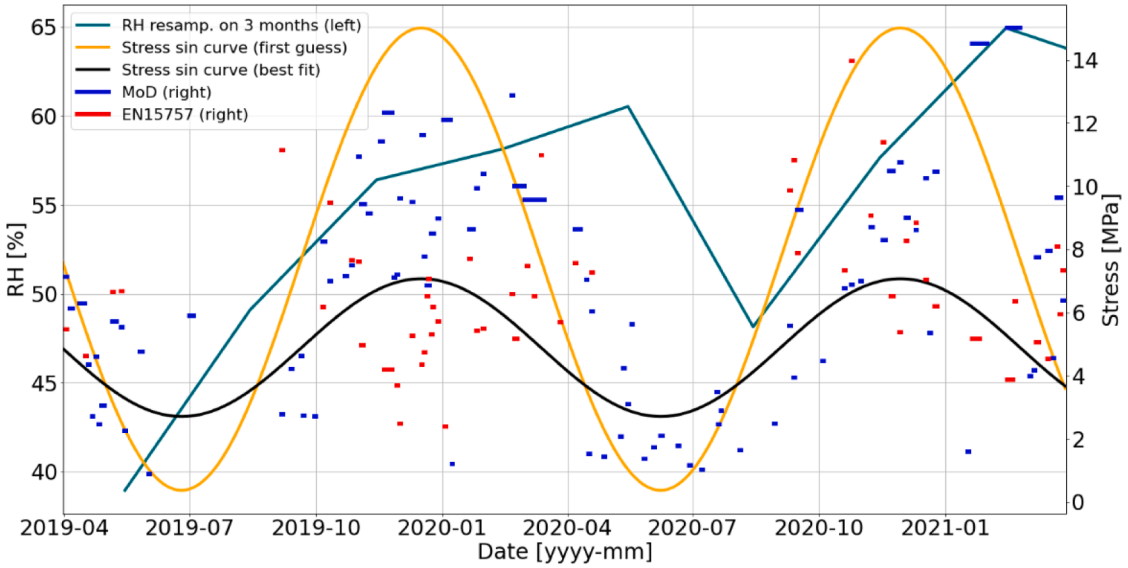

Fig. 13. Hygro-mechanical stress levels computed through the model in Section 2.3 for RH drops identified with the MoD strategy (blue segments) and with the EN15757 (red segments). The stress levels identified with the MoD strategy have been fitted through a sinusoidal curve (orange curve) with a period $T = 12$ months. The best fit of the sinusoidal curve (black curve) has been obtained through a least-squares optimization and follows a trend similar to that of the RH timeseries resampled with a frequency of three months (cyan curve).

the identified RH drops is shown in Fig. 10. In Fig. 10, on one hand, the orange points are representative of RH drops identified in the period in which the artificial heating is used in Ringebu church and, thus, they are due to the artificial conditioning of the indoor environment (heated drops); on the other hand, the purple points represent the RH drops identified in the period in which the artificial heating is not used and they are, therefore, due to the natural climate variability (natural drops). The black curve is a second order polynomial fit of the scattered data that perfectly catches the general trend. This means that a useful preliminary damage function can be expressed as follows:

$$S = \gamma(\Delta RH)^2 + \delta(\Delta RH) + \varepsilon \tag{15}$$

where S = level of hygro-mechanical stress in MPa, ΔRH is the experienced RH drop (in%), γ, δ, and ε are the quadratic fit parameters of the black curve in Fig. 10.

From Fig. 10 it can be easily noticed that the drops caused by the use of artificial heating could be severe in terms of hygro-mechanical stress, leading to possible fractures in the wooden objects surface that, with time, could propagate and cause catastrophic failures. All the collected data in terms of initial RH, final RH, ΔRH and stress can be used to build up a complete tool for assessing the hygro-mechanical risk for the wooden objects under concern, as visible in Fig. 11. The risk assessment tool (RAT) in Fig. 11 summarizes the effect of real hygric changes (collected from real monitoring data in Ringebu) on a slice of Scots pine, according to the experiments carried out in [21]. The boundary conditions are under the hypothesis that the slice of Scots pine, initially in equilibrium with the surrounding environment, is subjected to a sudden hygric drop. The final condition, after the change, lasts up to the achievement of the equilibrium of the object with the novel minimum in RH. In Fig. 11 on the *x*-axis the initial value of RH (named *RH start*) is reported, identified as the value from which the RH starts to decrease under the effect of a (natural or artificial) drop. On the *y*-axis the value of RH reached at the minimum of the drop (named *RH* min) is reported in a reversed order, identified as the local minimum of the RH timeseries. The light-gray dotted lines are isoΔRH lines representing the constant hygric change values going from ΔRH = 10% to ΔRH = 90%, while the black dashed lines are isostress lines representing constant stress levels going from σ = 2 MPa to σ = 12 MPa. The scatters shown in Fig. 11 represent the drops caused by the artificial heating (triangles) and by the natural microclimate (circles) that have been identified scanning the entire indoor RH timeseries measured in Ringebu following the MoD strategy described in Section 2.2 and Section 3.1. Therefore, each identified drop is positioned on the *RH* min *vs. RH start* plane, taking in consideration that, as a direct consequence, the experienced drop is ΔRH = RH start – RH min. Then, following the empirical procedure described in Section 2.3, the level of hygro-mechanical stress (in MPa) experienced for each RH drop has been evaluated and reported in Fig. 11 through colored scatters, associated to the color bar on the right. The colored regions, instead, have been delineated through experimental evidence in [21] and they highlight zones in which stress values and hygric changes cause: i) reversible (elastic) response in pine samples (green zone); ii) irreversible (plastic) response in pine samples (yellow zone); iii) fracture (gray zone).

It can be noticed that the increase in stress values and the increase in ΔRH have the same direction in terms of isolines, even if with different slopes. As a matter of fact, high values of stress occur even at low initial RH. When the slope increases, the risk of damaging the sample increases as well. This is explained by the cuneiform shapes of the reversible, irreversible and failure areas, which have their wedges towards low values of initial RH.

This means that RH drops characterized by low initial values of RH, although leading to moderate stress levels, are potentially dangerous because the narrow reversible and irreversible response areas could be easily crossed and the failure one could be entered. On the other hand, RH drops characterized by high values of initial RH, notwithstanding the capability of sweeping wide reversible and irreversible response areas before reaching the failure one, are perilous as lead to experiencing extremely high levels of stress (up to 14 MPa, in the current case). The novelty of the proposed RAT stands in several aspects. First, it is quite simple and – under its boundary conditions - allows to catch the main features of the impact of single, sudden and well determined RH drops in a single glance.

Second, it has been obtained by means of simplifying assumptions, leading to results that are physically plausible and easily readable even by non-experts in the field. In addition, the RAT allows to quickly identify and isolate risky conditions, to proceed in the direction of mitigating their effects by actuating the best conservation/preservation measures, namely decreasing the entity of the RH drops or managing the

starting and ending level of the RH in a better way.

As a matter of fact, it could be useful to establish a logic to avoid reaching too low values of RH by, for instance, controlling the use of artificial heating in cold months. Moreover, it is important to underline that the final RAT has been obtained starting from basic mathematical considerations Fig. 5, Eq. (7)-((14)) and passing through simple geometric functions (Fig. 6).

The levels of hygro-mechanical stress associated with each identified drops have been plotted over the two years of the monitored data in order to see their distribution over time (Fig. 12). In particular, in Fig. 12 there are the levels of stress computed following the model in Section 2.3 for the RH drops detected with the MoD strategy (blue segments) and the respective ones identified by the EN15757 (red segments). The length of each segment represents the duration of each drop, while the vertical position represents the level of stress identified through the right *y*-axis in Fig. 12. The stress levels have been plotted over the original indoor RH timeseries (a) and the same RH timeseries resampled with the following frequencies: one hour (b), twelve hours (c), one day (d), seven days (e), one month (f) and three months (g), in order to highlight possible matches between the periodicities of the RH timeseries and the stress timeseries. From Fig. 12 it can be easily noticed that the drops identified by the EN15757, being just the ones that cross the 7th percentile of the safe band (as described in Section 2.2), are confined in the periods when the artificial heating is used and, therefore, the RH fluctuations are more severe. On the other hand, the MoD strategy is able to catch even RH drops that are considered safe by the EN15757, namely those occurring when no artificial heating is in use and the microclimatic variability is mainly natural. Focusing on Fig. 12g, it can be highlighted that the blue segments follow, in some way, the trend of the cyan curve. This means that the stress levels associated with the MoDS drops are characterized, with good approximation, by a seasonal (*i.e.,* three months) variability. This is better visible in Fig. 13 where just the indoor RH timeseries resampled with a frequency of three months is reported (cyan curve). In addition, the segments representing the stress levels are shown as well, with the same meaning as in Fig. 12. Moreover, the first guessed sinusoidal fit of the blue stress levels (namely, those associated to the RH drops identified through the MoDS) is reported with an orange curve, while its best fit is reported with the black curve. Both sinusoidal curves have been obtained fitting only on the blue stress levels as the MoDS is able to detect almost every RH drop, allowing to build up a complete dataset. The orange curve has been obtained by computing a first-guess sinusoidal function in the form:

$$y = A\sin(\omega t + \varphi) + B \tag{16}$$

with a period $T = \frac{2\pi}{\omega} = 12$ months. The black curve has been obtained by optimizing the (16) through the least-squares method. Fig. 13 shows that the best-fit sinusoidal curve (black) follows, in some way, the timeseries of the indoor RH resampled with a frequency of three months, as previously noted. This further highlights that the stress levels are characterized, with reasonable simplifications, by a seasonal variability. As the RH drops occurring in autumn and winter are mainly due to the artificial heating that is turned on in case of scheduled events (celebrations, concerts, guided tours), the repeatability of these data may be questioned. In fact, it has been noticed that, despite exceptional cases (like, for example, the lockdown happened in 2020 due to the COVID-19 pandemic), the events are scheduled with a sort of repetitive pattern. This is witnessed both by metadata provided by the church's managers and by the RH drops identified in the timeseries. Therefore, the sinusoidal fit in Fig. 13 is useful as it shows that the total hygro-mechanical stress phenomenon can be assimilated to a low-frequency fluctuation [18].

In future perspectives, the just highlighted aspect can be used to study the fatigue effect on Scots pine wood caused by the repetition of stress history patterns. In addition, considering that each RH drop works like a single cycle of loading-unloading on the wooden samples/objects and that each of them has proper entity and duration, the entire drop timeseries could be seen as a variable-amplitude and variable-frequency loading history. By means of well-established models for fatigue cycle counting (*e.g.*, Rain-flow counting method [23]), the collected information could be useful for deeper investigations on the climatic fatigue behavior of Scots pine.

Once a variable loading history has been constructed, it could be possible to investigate the evolution of damage and fracture mechanisms over time. A reliable approach could be based on the Strain Energy Density (SED) method [24,25]. The SED method is a reliable and consolidated approach that allows performing parametric studies for evaluating the effect of different parameters on the strength of a component/structure/structural item both under static and fatigue loadings [26–28]. In particular, it has been widely used to assess the fracture of different kind of materials, showing to be highly versatile [29–31]. The SED method can represent, in this perspective, a fundamental tool to investigate the fracture behavior of historical materials, structures and artefacts. In addition, as it requires low computational resources, it may be used for establishing numerical campaigns aimed at simulating the fracture behavior of different wooden geometries subjected to single or repetitive hygric changes. The outcomes can help in improving the methodology, the damage function and the risk assessment tool presented so far and to broaden their field of applicability.

3.3. A preliminary machine learning approach

The models and algorithms described in Section 2.2, Section 2.3 and Section 3.1 allow to build up the RAT presented in Section 3.2. It has been obtained by carrying out evaluations on the monitored indoor RH timeseries and by setting up a model based on evidence available in literature. The RAT has shown to be useful, easy to obtain and to understand; moreover, it makes it possible to quickly evaluate the level of climate-induced risk experienced by wooden samples in terms of elastic, plastic, or failure response. However, a preliminary further step has been done towards the automatization of the entire modeling and procedure that allowed to reach the final aim of the work: understanding if the natural and artificial microclimate fluctuations (in terms of RH) could have detrimental effects on the conservation of historical wooden objects and building assets. In this framework, a first attempt has been made in implementing a machine learning (ML) algorithm that is able of predicting whether the wooden samples experience failure, based on analyzing brief chunks of microclimatic timeseries (indoor RH and T, outdoor RH and T). In detail, the problem under concern is a binary classification problem in which the final goal is to classify between two conditions: no failure (0) and failure (1). As eXtreme Gradient Boosting (XGBoost) machines [32] have shown to be highly reliable and robust in several fields, they have been chosen to carry out this preliminary test. The XGBoost classification model has been implemented in Python® language through the *sklearn* packages and it has been trained considering only data collected during the first year of the monitoring campaign (March 2019 – March 2020). In particular, six-hours-long chunks of indoor RH, indoor T, outdoor RH and outdoor T, ending at the t_{start} of each identified RH drop have been extracted from the entire timeseries. This means that for each RH drop, four timeseries chunks are available. Then, custom features for each timeseries chunks have been extracted, namely: the mean value, the median, the standard deviation,

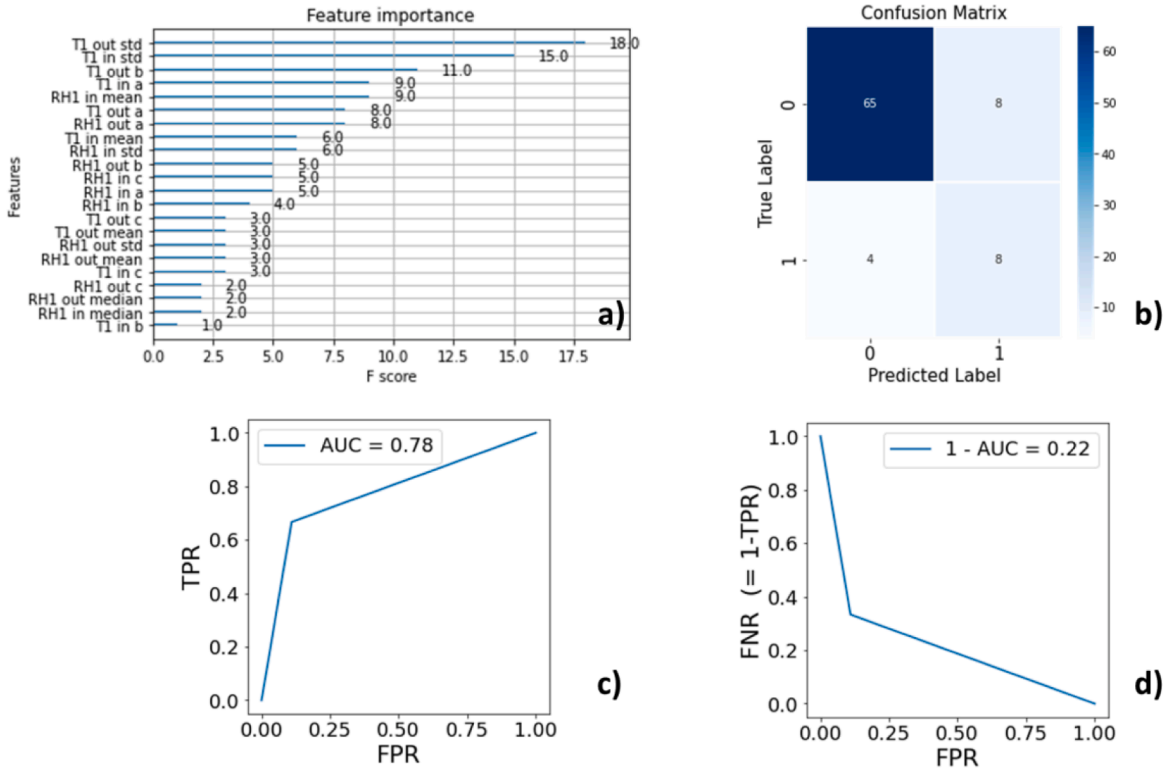

Fig. 14. Results of the XGBoost implementation: (a) bar plot of the importance of the training features; (b) confusion matrix of the test phase; (c) ROC curve for the test phase with its AUC; (d) complementary curve of the ROC with its area under the curve that is 1-AUC.

and the fit parameters (*a, b, c*) of the quadratic behavior that the chunks are assumed to qualitatively follow. Summarizing, for each identified RH drop twenty-four features are available (*i.e.*, six features for each of the four timeseries). These features are used as the input data for training the XGBoost classification model, while the provided output data are the labels (1 or 0) that define if each drop leads to failure or not, respectively.

As the desired output is a binary output, a logistic function has been

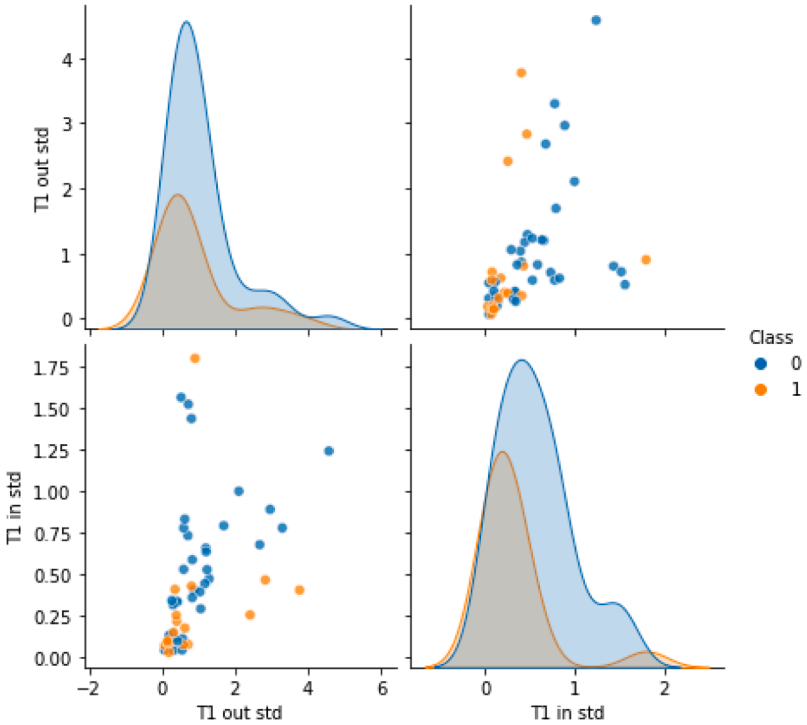

Fig. 15. Pair-plot of the most important features: T1 out std and T1 in std (as visible from Fig. 14a). The plots along the main diagonal are the univariate distributions for each feature for each label class (0 or 1), while the other two plots represent relationships between the two selected features.

set up as the objective function of the classification model and the Area Under the Curve (AUC) [33] has been chosen as evaluation metric for the model's performance. At the end of the training phase, the XGBoost classification model has gained a final AUC of about 0.80, which is fairly satisfactory.

After the XGBoost classification model has been trained, it has been tested on new unseen data: the ones collected during the second year of the monitoring campaign (March 2020 – March 2021). In particular, the same kind of data used for the training phase have been provided: twenty-four features for each identified RH drop. To evaluate the goodness of the XGBoost model, together with the Receiver Operating Characteristic (ROC) curve and AUC, the False Negative Rate (FNR) has been evaluated [33]. It is defined as

$$FNR = 1 - Recall = 1 - TPR \tag{16}$$

where TPR (True Positive Rate) and Recall are common scores adopted in this kind of evaluations [33]. The obtained results are reported in Fig. 14. In Fig. 14a bar plot of the importance of the training features is reported. The number "1″ near each feature's name represent the fact that the training data refer to the first year of the monitoring campaign. In Fig. 14a, the features are sorted in a decreasing order based on the *F-score*. This last score, in the current case, is computed as the number of times a feature appears in a decision tree. The higher the F-score, the heavier the feature in the decision process. From Fig. 14a the most relevant feature for the decision process of the implemented XGBoost model is the standard deviation of the outdoor temperature (*T1 out std*). This result is physically plausible; as a matter of fact, the most severe RH drops are those due to the use of artificial heating in the cold periods of the year. Since the use of artificial heating is strongly linked to the evolution of the outdoor temperature and to its variation, it is physically plausible that the standard deviation of the outdoor T influences the decision tree. In addition, according to Fig. 14a, the second most important feature is the standard deviation of the indoor T (*T1 in std*). Even in this case, the result is physically plausible as the indoor T depends on the outdoor T, both in case of artificial or natural microclimate. Fig. 14b shows the confusion matrix obtained for the test phase of the XGBoost classification model. The True 0 s (*i.e.*, real no failure events that are forecasted as no failures) are almost perfectly classified, while this does not happen for the True 1 s (*i.e.*, real failure events that are forecasted as failures). However, taking a look at Fig. 14c, it can be seen that an AUC of the ROC curve of about 0.78 is reached. As the maximum value that the AUC can reach is 1.00, the obtained outcome can be considered good, taking in consideration that this is just a preliminary and non-optimized attempt. In addition, the complementary curve of the ROC is reported in Fig. 14d, in which the FNR is made explicit. Keeping the FNR as low as possible is highly desirable; in point of fact, the false negatives (FN) are those features that are actually 1 s (*i.e.*, failure) but that have been predicted as 0 s (*i.e.*, no failure) by the algorithm. Therefore, the *FNR* is, in general, the portion of false 0 s. In the framework of preventive conservation, keeping low the portion of false 0 s is fundamental as they may cause underestimations of the actual risk induced by the drops of RH on the works of art. As seen in Fig. 14a, the two most important features for the decision process are the *T1 out std* and the *T1 in std*. These two features have reported in the pair plot in Fig. 15. The two plots on the main diagonal represent the univariate distribution of each feature for each label class (0 or 1, defined previously), while the two scatter plots represent the relationships between the two features. From Fig. 15 it can be noted that the two label classes are not well separated; as a matter of fact they often overlap in the different subplots. This is reflected in the results obtained in Fig. 14b, where the confusion matrix shows that the label classification can be surely improved. Summarizing, the preliminary results reported in Fig. 14 and Fig. 15 show that the preliminary implementation of machine learning approaches has provided promising results, since the training of the algorithm has been carried out by providing no information about the actual drops of RH.

In fact, the features used as input data have been computed on timeseries chunks that do not comprise the periods of time in which the RH drops occurred. Thus, despite having no information about the T and RH behavior in the drops time-windows, the chosen machine learning model has proven to be able to quite satisfyingly predict the possible failure (1) and non-failure (0) outcomes produced by the drops themselves.

4. Conclusions

In this work, the indoor microclimate of a wooden Medieval church (*i.e.*, Ringebu Church, located in Norway) has been analyzed. Studying the profile of relative humidity over a given period of observation is useful to notice the microclimatic variations that the church usually experience. In the field of preventive conservation, one commonly used RAT is the European Standard EN15757:2010; it has been established to provide guidelines for the assessment of historic microclimate of wooden objects/buildings that undergo variations in relative humidity. However, the provided indications are only useful to identify if risky RH fluctuations are in play, without supplying additional information about the entity of the experienced hygro-mechanical stress. For this reason, a simple novel algorithm (MoD strategy) has been proposed, based on scanning the entire set of data with the aim of identifying the actual RH variations. With some examples it has been shown that the proposed method is able of capturing the RH drops experiences by the case study in the period of observation. Then, a simple empirical model based on experimental and simulation evidence has been obtained in order to translate the hygric variations in levels of hygro-mechanical stress. In addition, a novel risk assessment tool (RAT), comprising all the information about the RH drops and the related stress levels, has been proposed, providing a quick way for identifying the mechanical evolution of the wooden objects subjected to microclimatic fluctuations. The profile of the hygro-mechanical stress over time has been observed, highlighting that it is a low-frequency phenomenon, which will be further deepened in the framework of the phenomenology of fatigue of wood. Finally, machine learning approaches have shown to be appealing for predicting the possible outcomes (1-failure or 0-non-failure) in case the wooden samples are subjected to unseen climatic scenarios. Near future perspectives will deal with the following aspects:

- including the time-response of wooden samples with respect to the timescales of RH drops. This way the effect of the duration of single or cumulated hygric changes on the mechanical decay of wood can be investigated;
- considering the entire stress history as a fatigue loading and modeling the fatigue behavior of wood, by taking into account the arising of different damage and fracture mechanisms over time;
- validating the proposed model with numerical simulations based on consolidated fracture mechanics approaches like the SED method;
- improving the machine learning approach by exploring other possible classification and prediction solutions; in particular, useful outcomes may be obtained by early predictions of future unseen scenarios in order to provide warning signals about the possible deformation and failure of wooden elements that may occur if no action is taken. Due to the extreme versatility of the proposed ML approach, it could be ideally extended to evaluations and predictions

on any kind of material and structure, becoming of general interest for the wide fields of fracture mechanics and structural integrity.

In conclusion, being aware of the possible stress and deformation fields that historical wooden materials may experience due to the natural and/or artificial microclimate is necessary for actuating the most effective conservation measures; for this purpose, both empirical and machine learning-based approaches have proven to be useful, as they allow easy and reliable evaluations of the climate-induced mechanical risk in hygroscopic materials.

Declaration of Competing Interest

The authors declare no conflicts of interest.

Acknowledgements

This work belongs to Sustainable Management of Heritage Building in a long-term perspective (Symbol) Research Project n. 274749 and to the Spara Och Bevara project n. 50049–1 and has been funded by the Swedish Energy Agency and the Norwegian Research Council, within a collaboration between the University of Padua (Italy) and the Norwegian University of Science and Technology NTNU (Norway). The authors are indebted to Dr. Elena Sesana for the hand drawing of Ringebu Stave church reported in Fig. 1b. The ownership of microclimatic data collected and used in this work is of the PI of the Symbol Project.

Appendix

Fig. A1a shows the measured indoor RH (blue curve), its moving average (MA) calculated over 30 days (black curve) and the 7th (bottom red curve) and 93rd (top red curve) percentiles of the RH fluctuations for Ringebu church, calculated according to [14], over two years of observation (from 30th March 2019 to 30th April 2021). In addition, the outdoor RH is plotted with a light gray curve. Fig. A1b shows the indoor T (orange curve) and the outdoor T (green curve) in Ringebu.

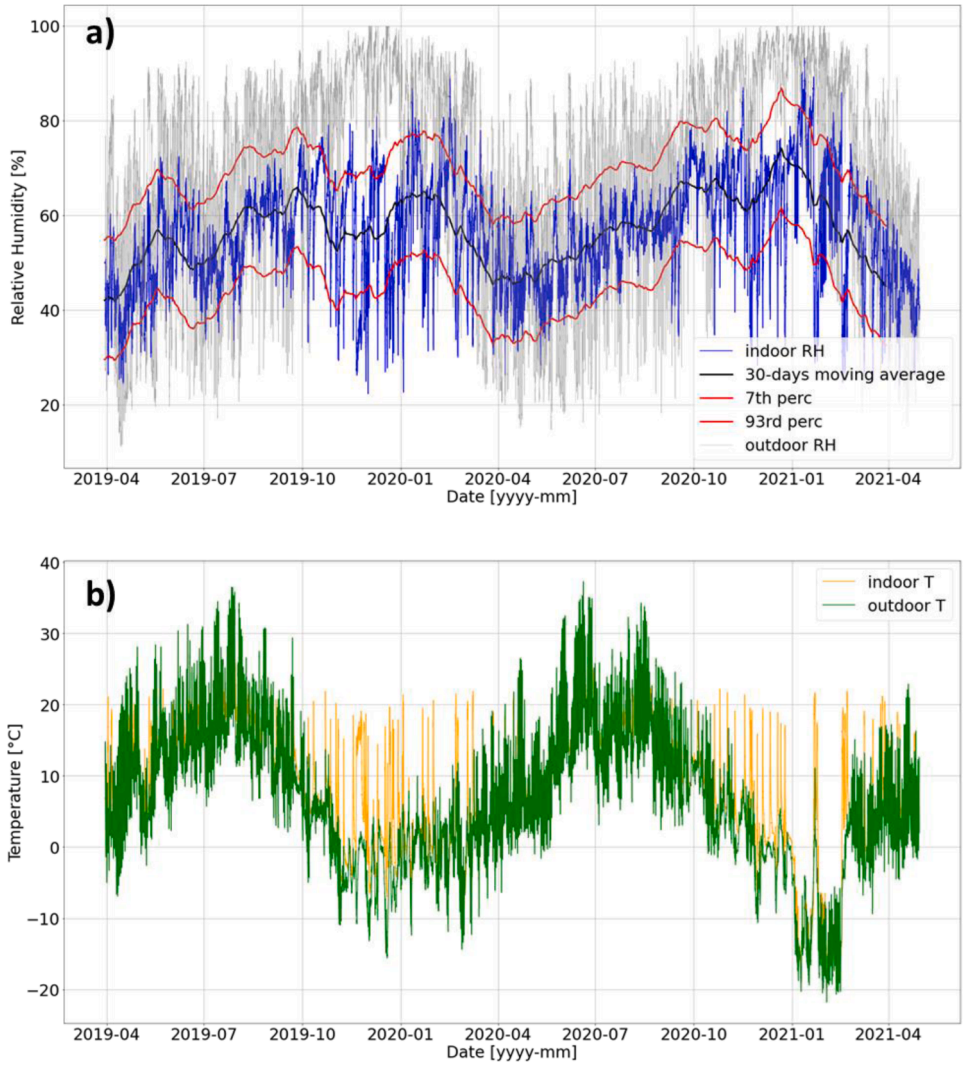

Fig. A1. Microclimatic timeseries collected inside and outside Ringebu church from the end of March 2019 to the end of April 202: (a) outdoor RH (gray), indoor RH (blue), moving average of RH (black) and percentiles (red) of RH fluctuations computed according to [14]; (b) outdoor T (green) and indoor T (orange).

References

[1] M.F. Mecklenburg, C.S. Tumosa, D. Erhardt, Structural Response of Painted Wood Surfaces to Changes in Ambient Relative Humidity, Paint. Wood Hist. Conserv. (1998) 464–483.
[2] D. Camuffo, Microclimate For Cultural Heritage, Elsevier Science, 2019.
[3] M. Andretta, F. Coppola, A. Modelli, N. Santopuoli, L. Seccia, Proposal for a new environmental risk assessment methodology in cultural heritage protection, J. Cult. Herit. 23 (2017) 22–32, https://doi.org/10.1016/j.culher.2016.08.001.

[4] UNI 10586-Condizioni climatiche per ambienti di conservazione di documenti grafici e caratteristiche degli alloggiamenti (1997).
[5] N. Aste, R.S. Adhikari, M. Buzzetti, S. Della Torre, C. Del Pero, H.E. Huerto C, F. Leonforte, Microclimatic monitoring of the Duomo (Milan Cathedral): risks-based analysis for the conservation of its cultural heritage, Build. Environ. 148 (2019) 240–257, https://doi.org/10.1016/j.buildenv.2018.11.015. October 2018.
[6] Dlgs 122/98 Art. 150 par6. Guideline on Technical and Scientific Criteria and standards of functioning and development of museum (2001).
[7] H.E. Silva, F.M.A. Henriques, Microclimatic analysis of historic buildings: a new methodology for temperate climates, Build. Environ. 82 (2014) 381–387, https://doi.org/10.1016/j.buildenv.2014.09.005.
[8] L. Bratasz, D. Camuffo, R. Kozlowski, Target microclimate for preservation derived from past indoor conditions, Museum Microclim (2007).
[9] D. Camuffo, E. Pagan, S. Rissanen, L. Bratasz, R. Kozlowski, M. Camuffo, A. DellaValle, An advanced church heating system favourable to artworks: a contribution to European standardisation, J. Cult. Herit. 11 (2) (2010).
[10] UNI 10829, Beni Di Interesse Storico e Artistico - Condizioni ambientali Di Conservazione - Misurazione ed Analisi, 1999.
[11] M.J. Varas-Muriel, M.I. Martínez-Garrido, R. Fort, Monitoring the thermal-hygrometric conditions induced by traditional heating systems in a historic Spanish church (12th-16th C), Energy Build. 75 (2014) 119–132, https://doi.org/10.1016/j.enbuild.2014.01.049.
[12] Ł. Bratasz, Allowable microclimatic variations in museums and historic buildings: reviewing the guidelines, 2012.
[13] H.E. Silva, G.B.A. Coelho, F.M.A. Henriques, Climate monitoring in World Heritage List buildings with low-cost data loggers: the case of the Jerónimos Monastery in Lisbon (Portugal), J. Build. Eng. 28 (2020) 24–35, https://doi.org/10.1016/j.jobe.2019.101029. June 2019.
[14] EN 15757 Standard - Conservation of Cultural Property - Specifications for temperature and relative humidity to limit climate-induced mechanical damage in organic hygroscopic materials, 2010.
[15] UNI EN 16893, Conservazione Del Patrimonio Culturale - Specifiche per La Scelta Del luogo, La Costruzione e Le Modifiche Di Edifici o Sale Finalizzate Al Deposito o All'esposizione Di Collezioni Del Patrimonio Culturale, 2018.
[16] ISO 19815, Management of the Environmental Conditions For Archive and Library Collections, 2018.
[17] American Society of Heating Refrigerating and Air-Conditioning Engineers, ASHRAE Handbook - HVAC Applications, 2011.
[18] W. Anaf, O. Schalm, Climatic quality evaluation by peak analysis and segregation of low-, mid-, and high-frequency fluctuations, applied on a historic chapel, Build. Environ. 148 (2019) 286–293, https://doi.org/10.1016/j.buildenv.2018.11.018. August 2018.
[19] H.L. Schellen, A.W.M. van Schijndel, Setpoint control for air heating in a church to minimize moisture related mechanical stress in wooden interior parts, Build. Simul. 4 (1) (2011) 79–86, https://doi.org/10.1007/s12273-011-0026-7.
[20] K.B. Ed, Preserving the Stave Churches: Craftsmanship and Research, 2022 n.d.
[21] C. Bertolin, P. Karvan, F. Berto, Natural climate stress caused by a hygric change on coated pine samples: theoretical formulation and experimental validation, Eng. Fail. Anal. (2021) 129, https://doi.org/10.1016/j.engfailanal.2021.105669.
[22] S. Jakieła, R.Kozłowski Bratasz, Numerical modelling of moisture movement and related stress field in lime wood subjected to changing climate conditions, Wood Sci. Technol. 42 (1) (2008) 21–37, https://doi.org/10.1007/s00226-007-0138-5.
[23] Y.L. Lee, T. Tjhung, Rainflow cycle counting techniques, Metal Fatigue Analysis Handbook (2012) 89–114.
[24] P. Lazzarin, R. Zambardi, A finite-volume-energy based approach to predict the static and fatigue behavior of components with sharp V-shaped notches, Int. J. Fract. 112 (3) (2001) 275–298, https://doi.org/10.1023/A:1013595930617.
[25] F. Berto, P. Lazzarin, A review of the volume-based strain energy density approach applied to V-notches and welded structures, Theor. Appl. Fract. Mech. 52 (3) (2009) 183–194, https://doi.org/10.1016/j.tafmec.2009.10.001.
[26] F. Berto, P. Lazzarin, Fatigue strength of Al7075 notched plates based on the local SED averaged over a control volume, Sci. China Physics, Mech. Astron 57 (1) (2014) 30–38, https://doi.org/10.1007/s11433-013-5275-2.
[27] P. Foti, S. Filippi, F. Berto, Fatigue assessment of welded joints by means of the strain energy density method: numerical predictions and comparison with eurocode 3, Frat. Ed Integrita Strutt. 13(47) (2019). https://doi.org/10.3221/IGF-ESIS.47.09.
[28] W. Song, X. Liu, F. Berto, P. Wang, H. Fang, Fatigue failure transition analysis in load-carrying cruciform welded joints based on strain energy density approach, Fatigue Fract. Eng. Mater. Struct. 40 (7) (2017) 1164–1177, https://doi.org/10.1111/ffe.12588.
[29] S.M.J. Razavi, M.R.M. Aliha, F. Berto, Application of an average strain energy density criterion to obtain the mixed mode fracture load of granite rock tested with the cracked asymmetric four-point bend specimens, Theor. Appl. Fract. Mech. 97 (2018) 419–425, https://doi.org/10.1016/j.tafmec.2017.07.004.
[30] F. Pegorin, A. Kotousov, F. Berto, M.V. Swain, T. Sornsuwan, Strain energy density approach for failure evaluation of occlusal loaded ceramic tooth crowns, Theor. Appl. Fract. Mech. 58 (2012) 44–50.
[31] M. Heydari-Meybodi, M.R. Ayatollahi, F. Berto, Rupture analysis of rubber in the presence of a sharp V-shape notch under pure mode-I loading, Int. J. Mech. Sci. (2018) 405–415, https://doi.org/10.1016/j.ijmecsci.2018.08.008, 146–147 (June).
[32] T. Chen, C. Guestrin, XGBoost: a scalable tree boosting system, in: Proc. ACM SIGKDD Int. Conf. Knowl. Discov. Data Min. 13-17-Augu, 2016, pp. 785–794, https://doi.org/10.1145/2939672.2939785.
[33] T. Fawcett, An introduction to ROC analysis, Pattern Recognit. Lett. 27 (2006).